What decides the size and composition of clay nano-aggregates in water? Charged polymers and multivalent ions competing in the formation of clay tactoids.

Claire Hotton, Anthony Beauvois, Pierre Levitz, Eric Ferrage, Thomas Bizien, Bruno Demé, Natalie Malikova, Laurent Michot

What decides the size and composition of clay nano-aggregates in water? Charged polymers and multivalent ions competing in the formation of clay tactoids

Claire Hotton[a,#1], Anthony Beauvois[a,#2], Pierre Levitz[a], Eric Ferrage[b], Thomas Bizien[c], Bruno Demé[d], Natalie Malikova[a,*] and Laurent Michot[a,*]

[a]PHENIX Laboratory, UMR 8234 CNRS, Sorbonne University, 75005, Paris, France

[b]Institut de Chimie des Milieux et Matériaux de Poitiers (IC2MP), CNRS, University of Poitiers, F-86073 Poitiers, France

[c] Synchrotron SOLEIL, l'Orme des Merisiers, 91190, Saint-Aubin, France

[d] Institut Laue Langevin (ILL), 71 Avenue des Martyrs, Grenoble, France

[#1]current affiliation : Univ Paris Saclay, CNRS, Lab Phys Solides, F-91405 Orsay, France

[#2]current affiliation : Synchrotron SOLEIL, l'Orme des Merisiers, 91190, Saint-Aubin, France

[*] corresponding authors: natalie.malikova@sorbonne-universite.fr, laurent.michot@sorbonne-universite.fr

Abstract

In this manuscript we address the formation of highly organized clay tactoids intercalated with a charged polymer (ionene) in aqueous environment. We report on an original route to achieve such tactoids by starting with pre-formed clay tactoids, held together by multi-valent inorganic atomic ions, as is the case in clay suspensions exchanged with Ca^{2+} or La^{3+} ions. Contrary to previously evoked mechanisms of disaggregation-aggregation or successive delamination of individual platelets ("peeling"), we observe clearly a reversible transition between the two types of clay tactoids, *at an almost constant number of clay nanoplatelets per tactoid*. This hints at an "earthworm" mechanism of the charged chains exchanging with the multivalent atomic ions inside the tactoids, which is surprising. Our observations are based on small angle X-ray scattering, where a strong correlation peak, called the stacking peak, is an undisputable signature of the stack/tactoid formation and is distinct for the multivalent-ion clay stacks and charged-polymer clay stacks. The linear charge density of the polymer chains is a key parameter for the tactoid transition. For weakly charged polymer chains, the transition simply does not take place, even under conditions of strong excess of the charged polymer. The initial state of multivalent-ion clay tactoids is essential for the formation of *highly organized* final charged-polymer clay tactoids. Starting from individual delaminated clay layers (Na^{+} exchanged clays) does not lead to the same final charged-polymer clay stacks. Overall, the final structure of charged-polymer clay stacks strongly depends on the initial structural state of the host clay layers, and on the linear charge density of the guest polymer chains.

1. Introduction

The coagulation/flocculation of clay minerals is a major process in various industrial applications. For instance, bentonite muds that are extensively used in civil engineering and oil drilling operations need to be processed by coagulation for a safe release of treated water into the environment [1]. Whereas simple inorganic cations can act as coagulating agents, the use of organic polymers and above all polyelectrolytes (charged polymers) generally provides a more efficient flocculation pathway [2]. Indeed, in addition to screening provided by an electrolyte, the presence of polyelectrolytes involves additional mechanism that are generally referred to as (i) polyelectrolyte bridging, (ii) polyelectrolyte patching, and, (iii) depletion flocculation involving the free, desorbed polyelectrolyte [3,4].

In all studies dealing with clay flocculation by polyelectrolytes, the charge density of the polymer appears as a key parameter controlling flocculation efficiency. For this reason, we recently focused on flocculation using ionene charged polymer chains. These molecules display a simple chemical structure, free of bulky side groups, and a regular charge density along the chains, as positive quaternary ammonium centers are separated by a predefined number of CH_2 spacer units [5-7], which allows tuning the linear charge density. The combination of ionenes of varying charge density, with clay platelets with different size and charge then appears as a very relevant system to study in detail the aggregation mechanisms of charged colloidal bidimensional objects.

In our first studies on this system, we investigated the aggregation of size-selected delaminated Na-exchanged clay platelets in the presence of ionene polymers using a combination of light absorbance, ζ-potential measurements and both X-ray and neutron small angle scattering techniques [8-9]. We could first show that the onset of efficient aggregation occurred for low ionene contents. More precisely, it appeared to be located at c^+/c^- values significantly lower than 1, where c^+/c^- is the ratio of the total positive charge on the ionene

chains and total negative charge on the clay platelets in the system. Still, differences in aggregation behaviour were observed depending on the relative charge density on the polymer chains and the clay surface. The nanoscale features of the formed clay aggregates were dominated by the presence of a stacking peak, giving clear evidence for a dominant face-to-face aggregation geometry of the clay platelets. The position and width of this stacking peak were shown to vary with the chain charge density of ionenes, highly charged chains leading to a flat conformation of the intercalated chains between clay platelets, whereas, for weakly charged chains, undulation of the intercalated ionene chains could be evidenced. In addition, the kinetics of clay-ionene aggregate or floc formation in the investigated systems, where ionene chains interact with freely moving individual charged clay platelets, appeared to be extremely quick (seconds to minutes).

However, in most real-life situations where clay minerals have to be flocculated, the initial clay system is very rarely the one in which individual platelets are present in suspension, as this requires the presence of monovalent counterions only and low ionic strength (typically $\leq 10^{-2}$ M/L) [*e.g.* 10]. In fact, in most "real" systems, where the compensating interlayer cation is multivalent, the initial clay particles are present as preformed stacks with repetition distances around 2nm that correspond to interlayers containing approximately 3 water layers. In the present paper we then examine how ionene polyelectrolytes with various charge densities interact with clay suspensions where already pre-formed clay tactoids are present, held together by multivalent inorganic cations, Ca^{2+} and La^{3+}. We show that for the case of pre-formed clay tactoids, the exchange of multivalent atomic ions and ionene polymer chains takes place only in certain cases. Even if the exchange takes place, it leads to different final aggregation states in comparison to ionene-induced aggregation of individual delaminated clay layers (the case of Na-exchanged clay suspensions). We give some indications regarding the mechanism via which the observed highly ordered clay-ionene aggregates are reached.

2. Experimental section

2.1. Clay preparation

The clay used in the present study is Na-Wyoming montmorillonite (SWy-2) that was obtained from the Source Clays Minerals Repository of the Clay Mineral Society at Purdue University. Clay suspensions were prepared, purified and size-sorted following the protocol described by Paineau *et al*. [11]. The size fractionation was performed by successive centrifugations and each obtained fraction has a defined platelet lateral size. In the present study, two different sizes were used. The physico-chemical parameters of the used clay samples are reported in Table 1. After size separation, the initial Na^+ clay counterions were exchanged with Ca^{2+} or La^{3+} using a 0.5 mol L^{-1} solution of $CaCl_2$ and a 0.1 mol L^{-1} solution of $La(NO_3)_3$, respectively. Salt solutions was added to the clay suspensions (≈ 20g/L) and stirred for 24h. The obtained mixture was then centrifuged at 7000 g during 30 minutes, the supernatant was eliminated and the flocculent was redispersed in the salt solution during 24h. These operations were repeated three times. After the third exchange, the suspensions were washed 10 times using ultrapure water in order to eliminate excess salts. The final ionic strength of the suspensions can then be estimated at around 10^{-4} mol L^{-1}.

Table 1 – Physico-chemical properties of studied clays [11, 12].

Name	Diameter nm	Polydispersity %	CEC mmol/100 g
SWy-2 S1	410	130	96.4
SWy-2 S3	100	45	96.4

2.2. Ionene preparation

Ionenes and their precursors were synthesized using a procedure adapted from those described previously [7, 13]. The first step in the synthesis is to prepare an aqueous solution of

Dimethylamine (DMA). For this, dimethylamine hydrochloride (86.0 g, 1.05 mol) was transferred in a two-necked, 500 mL round-bottom flask equipped with a magnetic stirrer. One neck was connected to a dropping funnel containing 23 M NaOH aqueous solution whereas the other one was connected to the tube immersed in ice-cold water (18 mL). NaOH was added dropwise to dimethylamine hydrochloride (DMA·HCl) under stirring at 10 °C. The mixture was warmed to its initial boiling point (55 °C) and then slowly further on up to 90 °C. DMA vapors condensed/dissolved while passing through ice-cold water. Such a procedure yielded an aqueous DMA solution (57%, 51.7 g, 0.63 mol) that was further used to synthesize N,N,N′,N′-tetramethyl-1,12-dodecanediamine. For this, 1,12-dibromododecane (8.35 g, 25 mmol) was dissolved in tetrahydrofuran (70 mL) in a 250 mL round-bottom flask. The solution was cooled to −78 °C, and aqueous solution of DMA (57%, 39.5 g, 0.5 mol) was added. After 30 min stirring at -78 °C, the reaction mixture was allowed to warm to room temperature and was stirred further for 24 h. Volatile components were removed under reduced pressure, and the resulting white residue was dissolved in 2 M NaOH aqueous solution (200 mL). The liquid phase was then extracted with diethyl ether several times. The combined organic layers were collected and concentrated to obtain a yellow oil. This crude product was purified via vacuum distillation (100 °C, 1 mbar) from CaH_2 to provide a clear colorless liquid product (4.5 g, 90% yield).

N,N,N′,N′-tetramethyl-1,12-dodecanediamine (4.5 g, 22.5 mmol) was added to a solution of 1,12-dibromododecane (5.77 g, 22.5 mmol) in methanol (55 mL). The reaction mixture was stirred for 3 days at 45 °C. The solution was then concentrated, and the residue was precipitated with diethyl ether. After decantation, the supernatant was eliminated. The remaining solid was then dissolved in water and washed with diethyl ether. After elimination of water by freeze-drying, 12,12-ionene was obtained as a white solid (12.49 g, 95%). As far as 6,6- and 3,3-ionene bromides are concerned, they were prepared similarly using the appropriate dibromoalkanes

and diaminoalkanes [6, 7, 14]. In the case of 3,3-ionene bromide, small amounts of water were repeatedly added into the reaction mixture, when it became white and very viscous, to ensure a proper solubility of all components. The structural characteristics of the three ionenes used are summarized in Table 2. As can be seen, the linear charge density of ionenes decreases as we move from 3,3- to 12,12-ionenes.

Table 2 – Structural characteristics of ionenes used. *Chain lengths of ionenes have been estimated from molecular weights as measured by size-exclusion chromatography. Further details can be found in refs [8,9].

Ionene	Structural formula of monomer $[-(CH_3)_2N^+-(CH_2)_x-(CH_3)_2N^+-(CH_2)_y-]_n$	Charge separation [Å]	Chain length* [nm]
3,3-	x=y=3	5.00	100-300
6,6-	x=y=6	8.75	100-300
12,12-	x=y=12	16.25	100-300

2.3. Clay-ionene floc preparation

Ionene aqueous solutions were prepared at 20 g L^{-1} for 3,3- and 6,6-ionene, and at 17 g L^{-1} for 12,12-ionene. Clay-ionene aggregates or flocs were prepared in test tubes to reach a final clay concentration of 11 g L^{-1}. c^+/c^- values of 0.4, 0.6, 0.8, 1.0, 1.2 and 2.0 were used where c^+ and c^- represent the concentration of positive charges from ionene and negative charges from clay platelets, respectively. Clay-ionene flocs were formed by adding the appropriate volume of the ionene solution to the clay suspension to reach the desired c^+/c^-. The mixture was shaken by hand, simply by inverting the test tube 2-3 times.

2.4. Small angle X-ray scattering

Small angle X-ray scattering (SAXS) measurements on equilibrated samples were performed on the SWING beamline at SOLEIL synchrotron (Orsay, France). Clay-ionene flocs were introduced into 1 mm cylindrical borosilicate capillaries that were sealed. The SAXS measurements were performed at a fixed energy of 16 keV using two sample-to-detector

distances, namely 0.5 and 6 m. This setup allowed covering a range of scattering vectors, q, from 0.002 $Å^{-1}$ to 2 $Å^{-1}$.

Kinetic SAXS experiments were carried out on a lab-based set-up (XENOCS Xeuss 2.0) at an incident energy of 8 keV. The sample to detector distance was fixed to 0.3m that corresponded to a q range of 0.02 $Å^{-1}$ to 1.2 $Å^{-1}$. Clay ionene suspensions were introduced into 1 mm cylindrical borosilicate capillaries immediately after mixing ionene with the clay suspension and analysed immediately. As the acquisition time was 60s, in such conditions, the first time at which a pattern is obtained can be estimated at around 3 minutes after the first contact between ionene and clay.

3. Results and discussion

3.1. High density ionenes.

Figure 1 displays the SAXS curves corresponding to flocs formed when SWy2-S1 initially exchanged with Na^+, Ca^{2+} or La^{3+} is contact with various amounts of 3,3-ionene expressed as C^+/C^-, *i.e.* the charge ratio between the charge corresponding to the positive charge on ionenes and the negative charge born by clay platelets. Note that until further notice, we describe here the larger clay platelets (410 nm in lateral size), denoted S1 (refer back to Table 1). The bottom panels are enlargements of the q-range between 0.2 and 0.6 $Å^{-1}$, *i.e.* the zone in which stacking peaks are observed. When the starting counterion is Na^+, as already observed [9], flocculation can be evidenced both in the high q range, where weak stacking peaks corresponding to repetition distances of around 15 Å appear upon ionene addition, and in the low q-range, where the initial q^{-2} dependence corresponding to the form factor (shape) of isolated clay platelets in suspension is replaced by a dual evolution (slope ≈ -2.8 for $q > \approx 3.10^{-2}$ $Å^{-1}$ and ≈ -2.5 for lower q values). The situation is strikingly different when the initial clay particles are exchanged with either Ca^{2+} or La^{3+} cations.

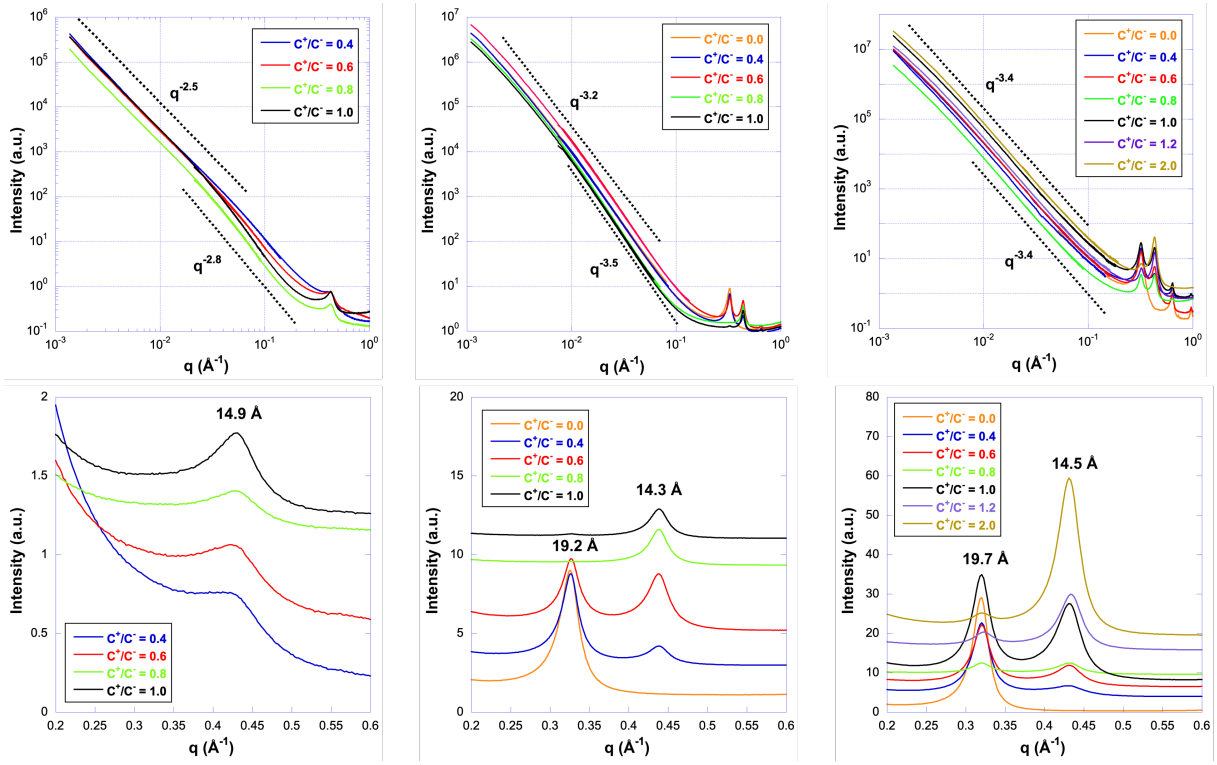

Figure 1: Evolution of the SAXS curves for SWy2-S1 in contact with increasing amounts of 3,3-ionene. Left Na^+-clay, middle Ca^{2+}-clay, right La^{3+}-clay.

Firstly, the total scattered intensity is significantly higher for the multivalent case. Secondly, in the region where the stacking of clay platelets is observed, the addition of ionene leads to the development of a peak corresponding to a repetition distance of ≈ 14.5 Å, *i.e.* a value close to that obtained upon flocculation of Na^+ clay. This peak seems to develop at the expense of the peak assigned to the initial Ca^{2+} or La^{3+} exchanged clay and grows in intensity with increasing ionene concentration. In the low q region, the slopes of the curves scale as $q^{-3.2}$ and $q^{-3.4}$ for the Ca^{2+} and La^{3+} systems, respectively. The assignment of these two peaks to inorganic cation exchanged stacks (or tactoids) and ionene exchanged stacks (or tactoids) is confirmed by measuring the signal of a dry floc at ambient atmosphere (Figure 1 SI). Indeed, in that case, two peaks are observed, one at ≈ 15.5 Å that corresponds to a clay with a water bilayer (as would be expected for a multivalent-ion clay tactoid at ambient humidity) and one at ≈ 14.3 Å that corresponds to a dry clay tactoid containing ionene. This additionally shows that ionene interlayers are very poor in water when present in aqueous environment. For each sample

prepared with multivalent-ion clay stacks, it is possible to determine an approximate number of platelets belonging to stacks with a repetition distance of ≈ 19 Å, *i.e.* containing hydrated multivalent cations or belonging to stacks with a repetition distance of ≈ 14 Å *i.e.* intercalated with ionene molecules. Such a calculation requires an estimation of the coherent scattering domain according to Scherrer's formula [9]:

$$CSD = \frac{0.89\,\lambda}{\beta \cos(\theta)}$$

where λ is the radiation wavelength, β the full width at half maximum of the diffraction peak and θ the diffraction angle.

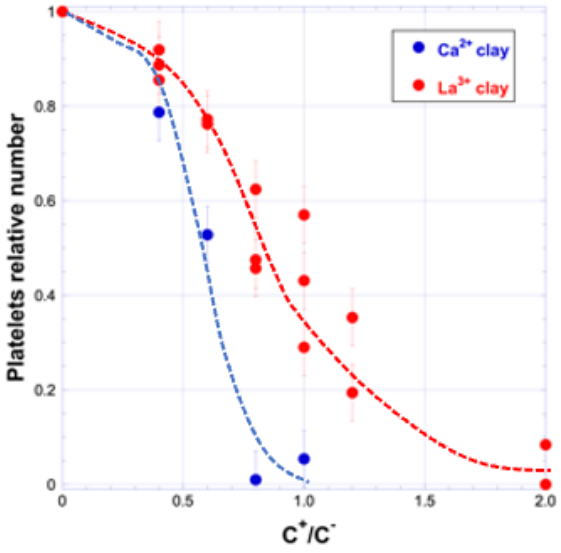

Figure 2: Evolution of the relative number of platelets in Ca^{2+} and La^{3+} SWy2-S1 stacks as a function of the amount of added 3,3-ionene, expressed in terms of the C^+/C^- ratio, a measure of relative concentration. Lines are guides to the eye.

Figure 2 displays the evolution with the ratio C^+/C^- of the relative number of platelets with a charge compensated with inorganic cations. It appears that this number tends to zero for both Ca^{2+} and La^{3+} samples for increasing ionene concentration. However, the amount of ionene required for reaching a complete exchange of the initial interlayer cation is significantly higher for La^{3+} counterions. The SAXS patterns of Figure 1 and the shape of the curves displayed in

Figure 2 suggest the occurrence in the system of a direct transition between two states, the "multivalent-ion stack" (abbreviated from now on as "m-ion stack") and the "ionene stack". To further test this assumption, it appears relevant to follow the evolution of the number of layers in the coherent scattering domain (CSD) for the various states of this transition (Figure 3). In the case of Ca^{2+}, (Figure 3A), the transition appears to occur at a constant number of clay layers per stack. In the case of La^{3+}, (Figure 3B), a slight evolution could be inferred.

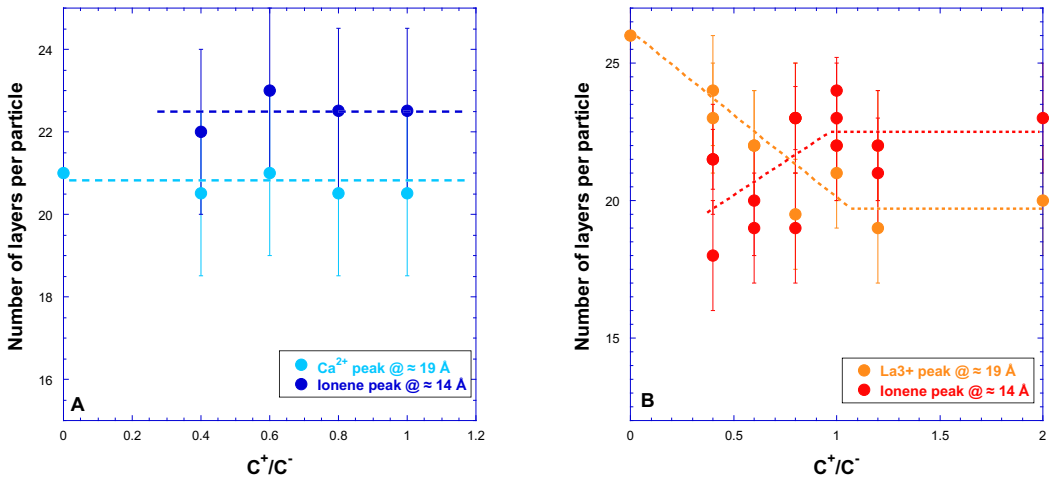

Figure 3: Evolution of the number of platelets per CSD in the two phases observed upon addition of 3,3-ionene to Ca^{2+} and La^{3+} SWy2-S1. Lines are guides for the eye.

However, considering the error associated with the exact determination of the number of layers from the measurement of the CSD, to a first approximation it can be proposed that in this case also, the number of layers per particles remains almost constant during the transition from "m-ion stack" to the "ionene stack". This strongly suggests that the exchange of inorganic multivalent cations by ionene chains occurs in structural units with a size that is fixed by the initial state of the sample.

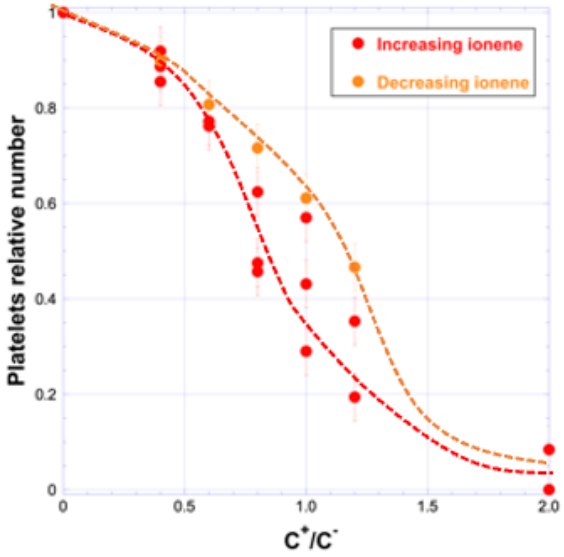

Figure 4: Evolution of the relative number of platelets in La^{3+} SWy2-S1 stacks as a function of the amount of added 3,3-ionene. Lines are guides for the eye.

It must be pointed out that such a result does not concur with the two classical models used for explaining polymer intercalation in swelling clay minerals, *i.e.* the disaggregation-reaggregation model [15, 16], or the peeling mechanism [16-18]. Indeed, both mechanisms assume at some point a change in the number of platelets per stack, which clearly does not apply to the systems investigated here, where a direct transition seems to occur. In order to get further insight into the status of this transition, it is important to check if the process is reversible. Figure 4 displays for the case of the La^{3+}- SWy2-S1 the evolution of the relative proportion of La exchanged platelets with both increasing and decreasing 3,3-ionene concentration. A small hysteresis between the two branches can be observed but clearly, the process appears reversible. This points towards a real phase transition between the two states, *i.e.* between the “m-ion stacks” and “ionene stacks”.

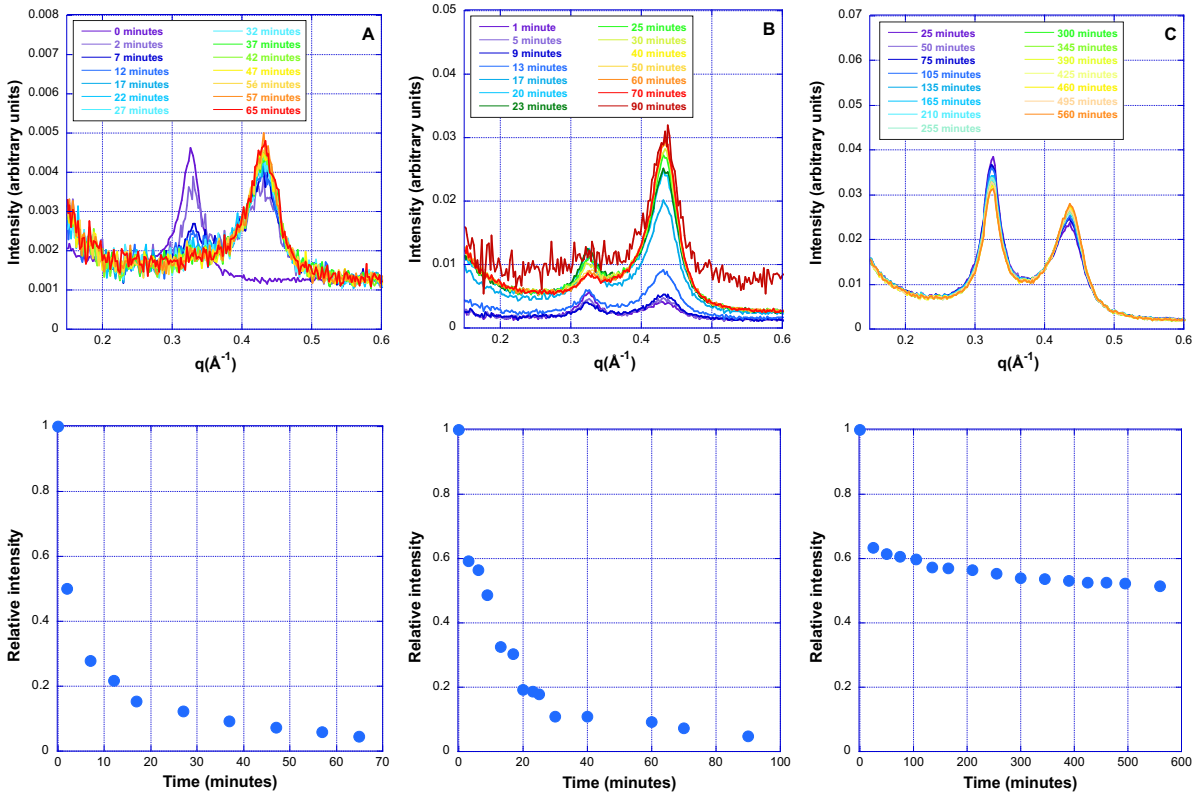

Figure 5: Time evolution of the integrated SAXS signals obtained for samples upon exchange with 3,3-ionene at a relative concentration C^+/C^- = 2. A: Ca^{2+} SWy2-S1, B: La^{3+} SWy2-S1, C: La^{3+} SWy2-S1 in a dense floc region.

In order to get further insight into the exchange mechanism between highly-charged ionene chains (3,3-ionene) and clays compensated by multivalent cations, kinetic experiments were carried out to follow the exchange process. Figure 5A presents the evolution obtained in the case of the Ca^{2+} SWy2-S1 for a relative concentration in ionene (C^+/C^-) equal to 2. Clearly the exchange process is rather slow, as it takes approximately one hour to obtain a full exchange between the two components, *i.e.* a full transition from "m-ion stacks" to "ionene stacks". The exchange in the case of La^{3+} exchanged sample appears slightly slower (Figure 5B). Furthermore, in the case of La-clay, Figure 5C presents the evolution of the signal measured in a dense region of the sample in which the signal/noise ratio is significantly higher than in less dense regions such as that observed in Figure 5B. In such dense regions, the evolution of the system appears to be even slower as the patterns keep evolving over periods of several hours. This suggests that accessibility and diffusion of ionene chains to preformed multivalent

moieties is of prime importance in such a system. It must be pointed out that after initial fast mixing in large vials, these kinetic experiments were carried out in 1mm SAXS capillaries, which may also slow down diffusion and render the homogenization of the system at these longer time scales difficult.

3.2. Effect of charge density.

Thanks to the use of model polyelectrolytes such as ionenes it is possible to get further insight into the exchange process by examining the effect of charge density, which turns out to be a key parameter. In the case of individual delaminated clay platelets (Na-exchanged clay), as shown in our previous study [9], the addition of ionenes leads to the formation of clay aggregates with d-spacings and coherent scattering domains that depend on the ionene charge density. It was observed that aggregates with d-spacings of 14.3 Å, 14.6 Å and 18.4 Å were formed for ionene 3,3- and 6,6- and 12,12 respectively. In parallel, the size of the coherent scattering domains corresponded to 11, 8 and 5 clay layers with decreasing ionene charge density. When the clays are initially exchanged with multivalent cations, the scenario is different. Indeed, with decreasing ionene charge density, the exchange of multivalent inorganic cations with ionene chains is impaired, be it for Ca^{2+} or La^{3+}. This is particularly striking when considering the ionene with the lowest charge density (12,12-ionene), for which no exchange of the inorganic atomic cations occurs whatever the amount of added ionene. Still, the tendency observed for 3,3-ionene holds for 6,6-ionene: the amount of ionene needed for reaching a given exchange ratio is lower for the Ca^{2+}-exchanged clay than for the La^{3+}-exchanged one.

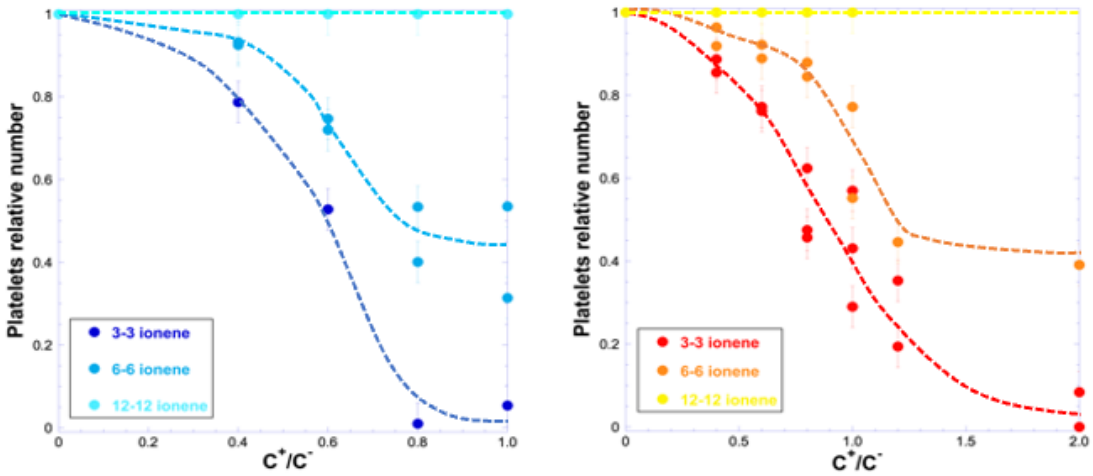

Figure 6: Influence of ionene charge density on the relative number of platelets with Ca^{2+} (left) and La^{3+}(right) Wyoming montmorillonite (all S1 platelets). Lines are guides to the eye.

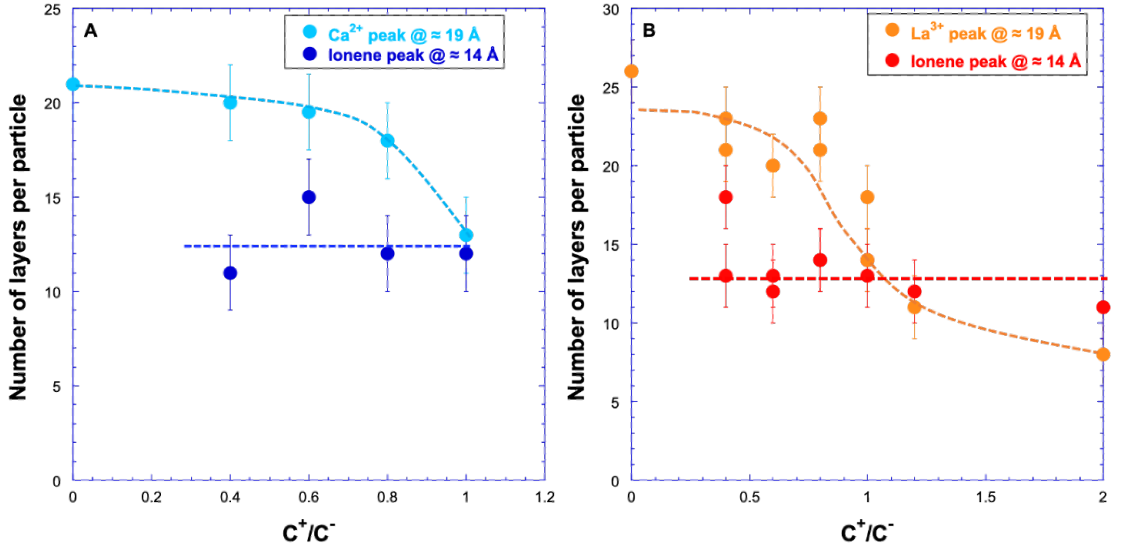

Figure 7: Evolution of the number of platelets per CSD in the two phases observed upon addition of 6,6-ionene to Ca^{2+} and La^{3+} SWy2-S1. Lines are guides to the eye.

As far as the number of platelets per CSD is concerned, as shown in Figure 7, the evolution in the case of 6,6-ionene bearing a medium charge density, is different from that observed for the highly charged 3,3-ionene (Figure 3). Indeed, the number of platelets in the aggregates of "6,6-ionene-clay stacks" is constant at around 13, a value significantly lower than that observed for the 3,3 ionene case (≈ 22). It then appears that the final state of the stack is linked to the charge density of the interlayer chain.

Figure 8 displays the kinetic evolution of the system involving Ca^{2+} SWy2-S1 and La^{3+}SWy2-S1 and 6,6-ionene. As in the case of the 3,3-ionene, kinetics are rather slow with exchange time extending over a few hours or even more. The kinetics may be slightly slower than those observed with the higher charge density chains (3,3-ionene). However, reproducing the same local conditions in such an experiment is rather difficult, which somewhat mitigates the statement.

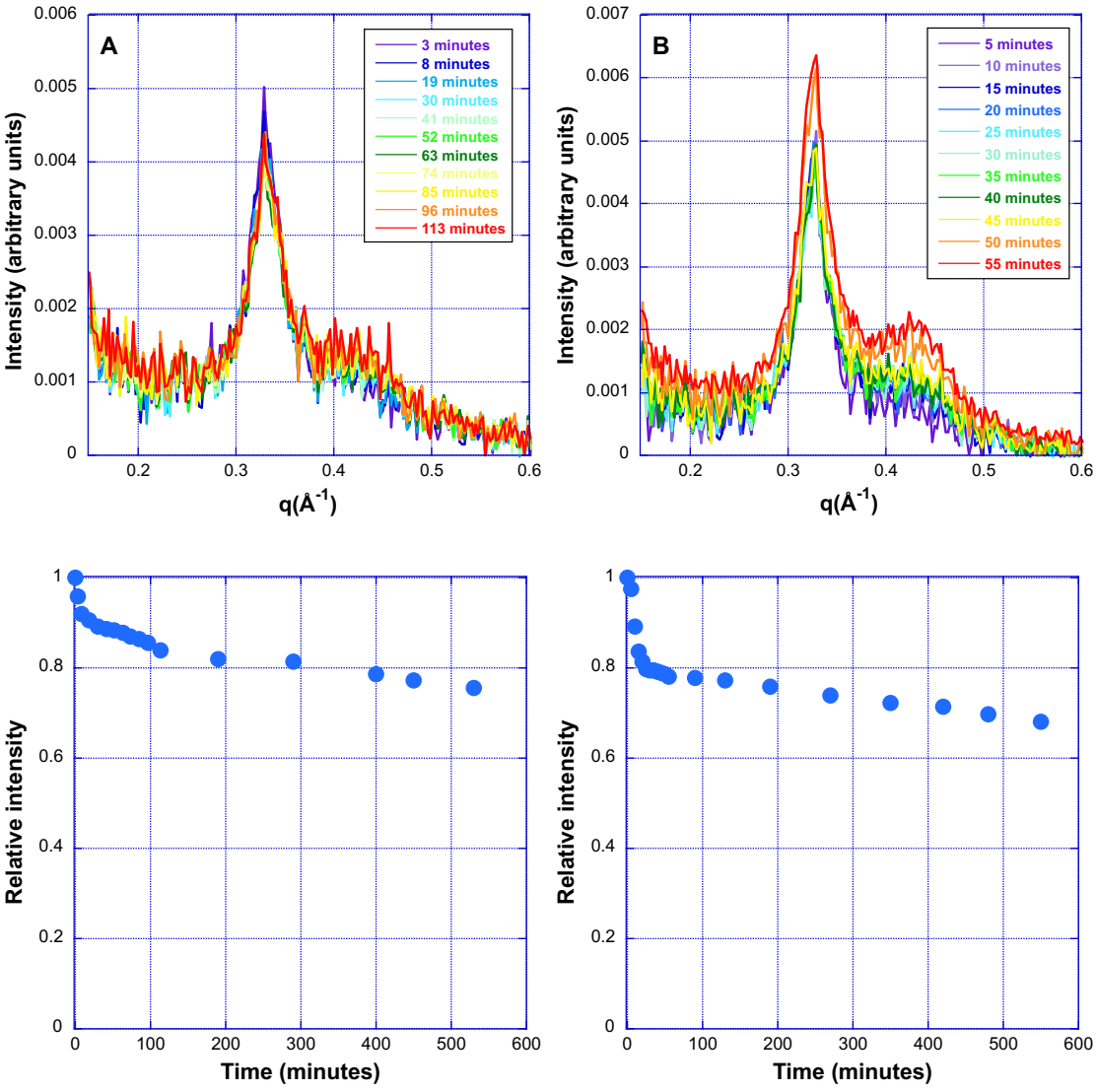

Figure 8: Time evolution of the integrated SAXS signals obtained for samples upon exchange with 6,6-ionene at a relative concentration C^+/C^- = 2. A: Ca^{2+} SWy2-S1, B: La^{3+} SWy2-S1.

It is worth noting that the average particle size of clays seems to have only a marginal influence on the equilibrium state (Figure SI2) as well as on the kinetics of its formation (Figure

SI3). The system appears to behave indeed similarly for the two clay particle sizes investigated, 410nm (S1) and 100nm (S3).

All the data presented here strongly suggest that the exchange of charged polymers in clay suspensions strongly depends on both the initial state of the clay component and the charge density of the guest polymer molecule. In the case of Na-clay where the initial state of the system is that of individual clay layers dispersed in suspension, whatever the charge density of the guest molecule, exchange occurs. Still the final state of the sample depends on the charge density of the introduced polymer [8,9]. When the initial clay sample is exchanged with multivalent cations, only ionenes with sufficiently high charge density (3,3- and 6,6-ionenes) are able to exchange the multivalent cations in the preformed "M-ion stack" structure. For 3,3-ionenes, the exchange kinetics and the evolution of the scattering coherent domains throughout the exchange curves strongly suggest a pure reptation of the polymer chains into the preformed "M-ion stack", the structure of which remains similar all along the exchange process. For 6,6-ionenes, kinetics also points towards some kind of "earthworm" mechanism. However, the final state of the sample is slightly different from the initial one as the average number of layers per stack in the "ionene stack" is slightly lower than in the "M-ion stack". It then appears that the equilibrium state of stacked clay structures formed upon charged polymer intercalation depends on a subtle match between the charge density of the host structure and that of the guest species, in addition to the initial state.

4. Concluding remarks

The results presented in this paper show that the interaction of model charged polymer chains, with variable linear charge density, with particles of Wyoming montmorillonite leads to final structures that strongly depend on the initial structural state of the host layers, and on the linear charge density of the guest polymer chains. Exchange does not seem to occur through the

mechanisms currently proposed in the literature, *i.e.* disaggregation-reaggregation or peeling. In the case where pre-formed clay tactoids exist, some "earthworm" type mechanism appears to be more appropriate for describing the structural and kinetic evolution of the structures with increasing polymer concentration. Furthermore, the final equilibrium state of stacked clay structures formed upon charged polymer intercalation seems to depend on a subtle match between the charge density of the host structure and that of the guest species. In that context, considering the charge heterogeneity of natural clay minerals, the evolution of the system upon increasing polymer addition could be a proxy for the charge distribution of the ensemble of clay layers. In that regard and to see whether this balance controls all clay systems for which stacks of particles are present it would be extremely fruitful to reproduce the experiments done in the present study using other natural clays with different charge and/or charge distribution or to use synthetic clay systems with controlled charge density. Performing simulations such as those described in [19, 20] could also help in better assessing the processes occurring when charged polymers are in contact with various types of clay stacks or tactoids. All these investigations could undoubtedly lead to a more efficient design of clay-polymer nanocomposites for all kinds of applications.

5. Acknowledgements

We acknowledge the financial support of the Institute of Materials (iMat) of Sorbonne University (SU, Paris, France) for the post-doctoral position of Anthony Beauvois. The authors acknowledge the SOLEIL synchrotron (Saint-Aubin, France) for awarding beamtime for SAXS experiments on beamline SWING (as part of the block-allocation-groups (BAG) 20201118 and 20221057), Institute Laue Langevin (Grenoble, France) for test measurements on the diffraction beam-line D16 and Federation Chimie Materiaux Paris Centre of SU for beam-time on the XEUSS 2.0 SAXS instrument, an SU platform.

6. References

[1] Chandan, K.K, Karmakar, G.P. (2019) Drilling fluid waste treatment using polysaccharide-grafted copolymers. The APPEA Journal 59, 34–46

[2] Bratby, J. (1980). "Coagulation and flocculation. With an emphasis on water and wastewater treatment." (Uplands Press Ltd: Croydon)

[3] Bolto, B., Gregory, J. (2007) Organic polyelectrolytes in water treatment. Wat. Res. 41, 2301-2324

[4] Schwarz, S. and Petzold, G. (2014) Polyelectrolyte Complexes in Flocculation Applications. Advances in Polymer Science, 256, 25-65.

[5] Noguchi, H., Rembaum, A. (1969) Ionene polymers. II. Formation ofcyclic and linear compounds or polymers from N,N,N′,N′-tetramethyl-α,ω-diaminoalakanes and α,ω-dibromoalkanes. J. Polym. Sci., Part B: Polym. Lett. 7, 383−394.

[6] Malikova, N., Čebašek, S., Glenisson, V., Bhowmik, D., Carrot, G., Vlachy, V. (2012) Aqueous solutions of ionenes: Interactions and counterion specific effects as seen by neutron scattering. Phys. Chem. Chem. Phys. 14, 12898−12904.

[7] Malikova, N., Rollet, A.-L., Čebašek, S., Tomšič, M., Vlachy, V. (2015) On the crossroads of current polyelectrolyte theory and counterion specific effects. Phys. Chem. Chem. Phys. 17, 5650−5658.

[8] Sakhawoth, Y., Michot, L.J., Levitz, P., Malikova, N., 2017. Flocculation of Clay Colloids Induced by Model Polyelectrolytes: Effects of Relative Charge Density and Size. ChemPhysChem 18, 2756–2765.

[9] Sakhawoth, Y., Michot, L.J., Levitz, P., Rollet, A-L., Sirieix-Plenet, J., Hermida Merino,D., Malikova N. (2019) Aggregation of Plate-like Colloids Induced by Charged Polymer Chains:

396 Organization at the Nanometer Scale Tuned by Polymer Charge Density. Langmuir, 35,
397 10937−10946
398 [10] Michot, L. J., Bihannic, I., Porsch, K., Maddi, S., Baravian, C., Mougel, J., Levitz, P.
399 (2004) Phase diagrams of Wyoming Na-montmorillonite clay. Influence of particle anisotropy.
400 Langmuir 20, 10829−10837.
401 [11] Paineau, E., Bihannic, I., Baravian, C., Philippe, A.-M., Davidson, P., Levitz, P., Funari,
402 S.S., Rochas, C., Michot, L.J., 2011. Aqueous Suspensions of Natural Swelling Clay Minerals.
403 1. Structure and Electrostatic Interactions. Langmuir 27, 5562–5573.
404 [12] Michot, L.J., Bihannic, I., Maddi, S., Baravian, C., Levitz, P., Davidson, P., 2008. Sol/Gel
405 and Isotropic/Nematic Transitions in Aqueous Suspensions of Natural Nontronite Clay.
406 Influence of Particle Anisotropy. 1. Features of the I/N Transition. Langmuir 24, 3127–3139.
407 [13] Čebašek, S., Serucnik, M., Vlachy, V. (2013) Presence of hydrophobic groups may modify
408 the specific ion effect in aqueous polyelectrolyte solutions. J. Phys. Chem. B, 117, 3682−3688.
409 [14] Čebašek, S., Lukšic, M., Pohar, C., Vlachy, V. (2011) Thermodynamics of dilution and
410 the Hofmeister series in aqueous solutions of aliphatic ionenes with halide counterions. J.
411 Chem. Eng. Data, 56, 1282−1292.
412 [15] Larsson, N., Siffert, B. (1983) Formation of lysozyme-containing crystals of
413 montmorillonite. Journal of Colloid Interface Science 93, 424–431.
414 [16] Lagaly, G., Ogawa, M., Dekany, I. (2006) Clay Mineral organic interactions Chapter 7.3
415 in Handbook of Clay Science F. Bergaya, B.K.G. Theng and G. Lagaly eds Developments in
416 Clay Science, Vol. 1 Elsevier Ltd.
417 [17] Billingham, J., Breen, C., Yarwood, J. (1997) Adsorption of polyamine, polyacrylic acid
418 and polyethylene glycol on montmorillonite: an in-situ study using ATR-FTIR. Vibrational
419 Spectroscopy 14, 19–34.
420 [18] Breen, C., Rawson, J.O., Mann, B.E., 1996. Adsorption of polycations on clays: an in situ

421 study using 133Cs solution-phase NMR. Journal of Materials Science 6, 253–260.
422 [19] Thuresson, A., Segad, M., Plivelic, T. S., Skepö, M. (2017) Flocculated Laponite-
423 PEG/PEO Dispersions with Multivalent Salt: A SAXS, Cryo-TEM and Computer simulation
424 Study, J. Phys. Chem. C, *121*, 7387-7396.
425 [20] Jansson, M., Belić, D., Forsman, J., Skepö, M. (2020) Nanoplatelet interactions in the
426 presence of multivalent ions: The effect of overcharging and stability, J. Coll. Interface Sci.
427 579, 573-581.
428